

# Mega-Pixel Detector Arrays: Visible to 28 $\mu\text{m}$

Alan W. Hoffman\*, Peter J. Love, and Joseph P. Rosbeck  
Raytheon Vision Systems, Goleta, CA, USA

## ABSTRACT

Large infrared detector arrays are now available that meet the demanding requirements of the astronomy and civil space communities. This paper describes arrays with more than one million detector elements developed by Raytheon Vision Systems for these low-background applications. These detector arrays have 1024 x 1024 and 2048 x 2048 formats with element spacing ranging from 20 to 27  $\mu\text{m}$ . Arrays of this size have been demonstrated with a variety of detector materials: Si PIN, HgCdTe, InSb, and Si:As IBC. The performance of each of these materials on arrays with more than one million detector elements is discussed. All of these detector materials have demonstrated low noise and dark current, high quantum efficiency, and excellent uniformity. All can meet the high performance requirements for low-background within the limits of their respective spectral and operating temperature ranges. Features of the readout integrated circuits that mate to these detector arrays are also discussed.

Companion papers in these SPIE proceedings that discuss several of these arrays in more detail are:

- "Large-format 0.85 and 2.5  $\mu\text{m}$  HgCdTe detector arrays for low-background applications," P. J. Love, A. W. Hoffman, D. L. Gulbransen, K. J. Ando, M. P. Murray, N. J. Therrien
- "James Webb Space Telescope characterization of flight candidate NIR InSb array," C. W. McMurtry, W. J. Forrest, J. L. Pipher, A. C. Moore
- "Orion II: the second-generation readout multiplexer for largest infrared hybrid focal plane," K. M. Merrill, A. M. Fowler, W. Ball, A. Henden, F. J. Vrba, C. McCreight
- "Interpixel capacitance in nondestructive focal plane arrays," A. C. Moore
- "Radiation environment performance of JWST prototype FPAs," M. E. McKelvey, K. A. Enico, R. E. McMurray Jr., R. A. Reed, C. R. McCreight
- "Independent testing of JWST detector prototypes," D. F. Figer, B. Rauscher, M. W. Regan, J. Balleza, L. Bergeron, E. Morse, H. S. Stockman

Keywords: low-background, infrared, detector, readout, Si PIN, HgCdTe, InSb, Si:As, IBC

## 1. INTRODUCTION

Several types of systems have consistently desired larger detector arrays to better accomplish their goals. Astronomers in particular have eagerly waited for the day when electronic arrays could match the size of photographic film. Over the past 20 years astronomy has led the development of larger visible, as well as infrared arrays. Infrared arrays are now available for astronomy and other low-background applications that exceed one million ( $1 \times 10^6$ ) detector elements (pixels) and, for the largest infrared arrays yet made, over four million ( $4 \times 10^6$ ) pixels.

Two manufacturers of infrared detectors are currently making arrays of one million pixels or greater for low background applications, Raytheon Vision Systems and Rockwell Scientific. These arrays are manufactured as a hybrid structure, often called a sensor chip assembly (SCA), which consists of a detector array connected with indium bumps to a readout integrated circuit chip (ROIC). Raytheon has developed 1024 x 1024 arrays with detector element sizes of 20, 25, and 27  $\mu\text{m}$  and 2048 x 2048 arrays with element sizes of 20 and 25  $\mu\text{m}$ . Raytheon has demonstrated large format in a variety of detector materials: Si PIN, SWIR HgCdTe, MWIR HgCdTe, InSb, and Si:As IBC. A discussion of the spectral ranges and operating temperatures of these detectors is found in the following section.

---

\* ahoffman@raytheon.com; phone: 805-562-2230; fax: 805-562-2127

## 2. DETECTOR ARRAY CHARACTERISTICS

The spectral ranges of five high performance detector materials suitable for low-background applications are shown in Figure 1. These materials are Si PIN, SWIR HgCdTe, MWIR HgCdTe, InSb, and Si:As IBC. Where the background and signal photon fluxes are very low, detector noise and detector dark current must also be very low. The detector temperature must be correspondingly low in order to achieve the low dark current. The operating temperature range of each of the detector materials is shown in Figure 1 with a dashed line that indicates the general trend that the longer cutoff wavelength of the detector generally requires a lower operating temperature to achieve the same dark current performance. The operating temperature range indicated in Figure 1 are fairly broad due to the wide range of system backgrounds.

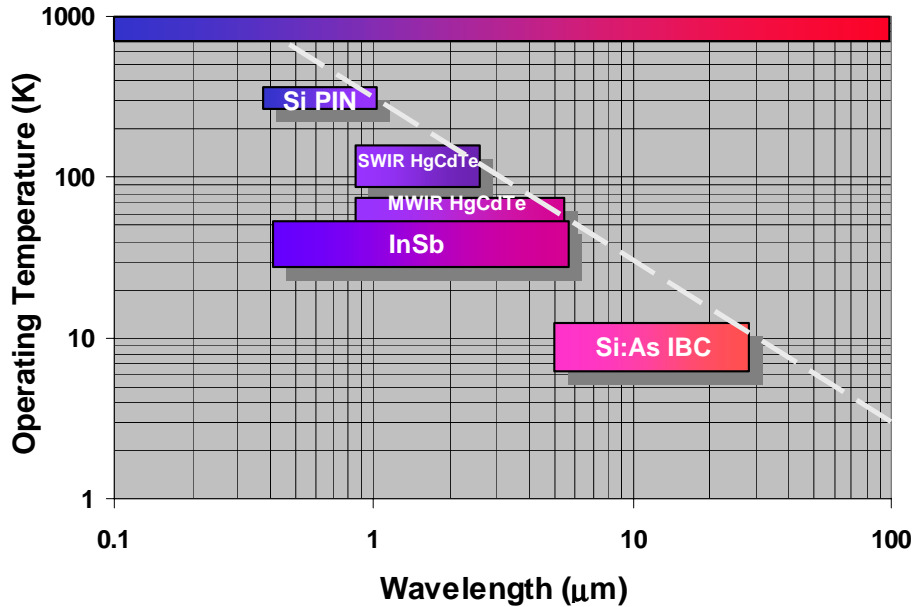


Figure 1. High-performance detector materials available at Raytheon. Operating temperatures for low-background systems is shown for each material along with the spectral band of greatest sensitivity. The dashed line indicates the trend toward lower operating temperature for longer wavelength detection.

### 2.1 Si PIN detectors

Si PIN detectors operate in the visible (optical) wavelengths and into the NIR as indicated in Figure 2. The main features of Si PIN detectors in a hybrid/SCA format are: high quantum efficiency, especially at the NIR end of the spectrum; nearly 100% fill factor, since the electronic circuitry is on a separate chip and does not block the incoming radiation; and high radiation tolerance compared to CCDs, since the detector and the CMOS readout are both inherently tolerant. While arrays up to 4K x 4K are feasible with current technology, the largest format demonstrated for astronomy is a 1K x 1K (1024 x 1024) which is shown in Figure 3.

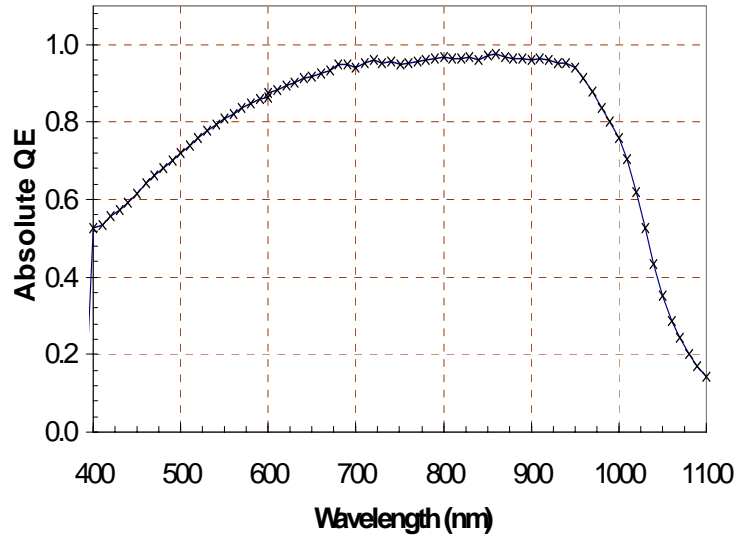


Figure 2. Spectral response of a typical Si PIN detector showing absolute quantum efficiency (QE) plotted against wavelength. The high QE in NIR is a feature of Si PIN detectors in hybrid/SCA structures.

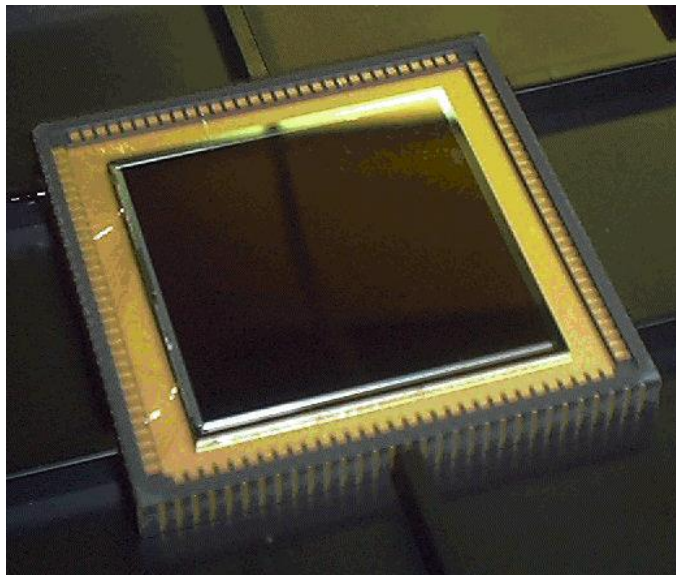


Figure 3. Photo of a 1024 x 1024 Si PIN SCA in a standard leadless chip carrier (LCC) package

## 2.2 HgCdTe detectors

The bandgap, and therefore the cutoff wavelength of HgCdTe, can be adjusted by varying the atomic ratios during crystal growth. By the definition of the infrared industry, SWIR HgCdTe has a cutoff wavelength between 1.7 and 3.2  $\mu\text{m}$ . Typical spectral curves of three Raytheon HgCdTe detectors are shown in Figure 4. The absolute QE for this material is 70 to 80% for detectors with no antireflection (AR) coating and typically 80 to 95 % with an AR coating. The cuton wavelength of 0.85  $\mu\text{m}$  is determined by the CdZnTe substrate, which can be removed to extend the spectral response further into the visible.

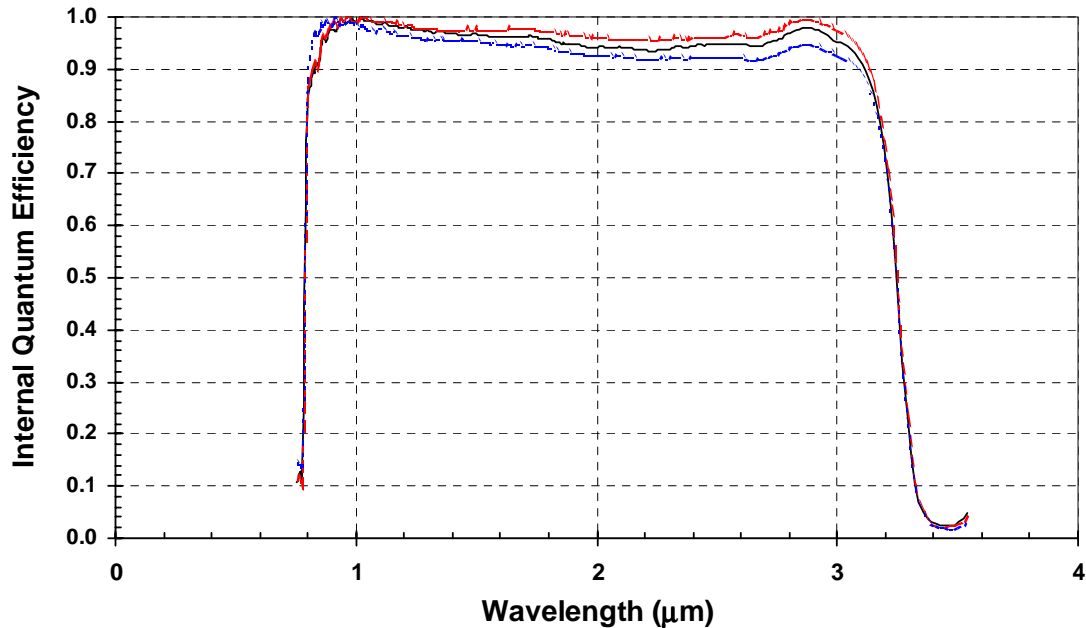


Figure 4. Spectral response of a typical SWIR HgCdTe detector showing internal QE plotted against wavelength. The cuton wavelength is determined by the transmission of the CdZnTe substrate while the cutoff is determined by the Hg to Cd ratio. The high QE even at the shortest wavelengths is a feature of Raytheon's HgCdTe structure.

SWIR HgCdTe SCAs have been demonstrated in both 1024 x 1024 and 2048 x 2048 formats. Figure 5 shows the 2048 x 2048 Virgo SCA, which is currently being manufactured for the UK's VISTA telescope. The readout associated with this SCA can be operated with either 4 or 16 output lines and has demonstrated total noise of 18e- in CDS (correlated double sample) mode with detectors attached.<sup>1</sup>

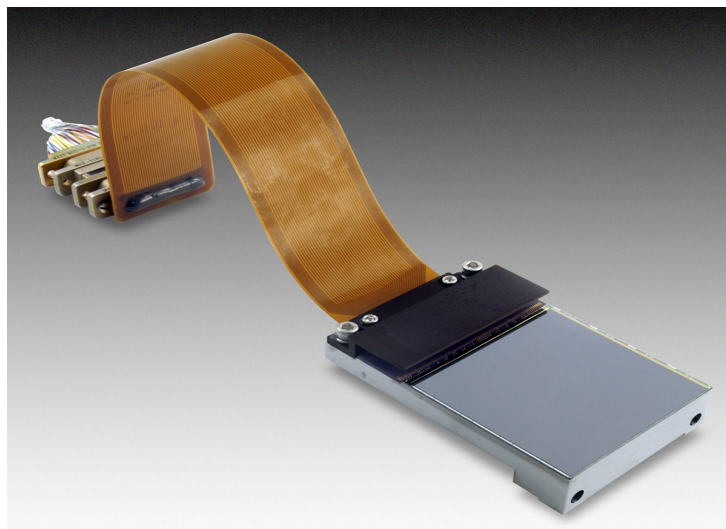


Figure 5. Photo of a 2048 x 2048 Virgo SWIR HgCdTe SCA mounted on a module. The module consists of a precision metal pedestal, an electrical interface cable, and a temperature sensor.

Raytheon MWIR HgCdTe detectors, which exhibit cutoff wavelengths around 5  $\mu\text{m}$ , have a uniform spectral response as shown by the data from three detectors in Figure 6. The QE for non-AR coated detectors is around 80%. These detectors were selected for the VIRTIS instruments on the European Space Agency's Rosetta mission, which is awaiting launch.

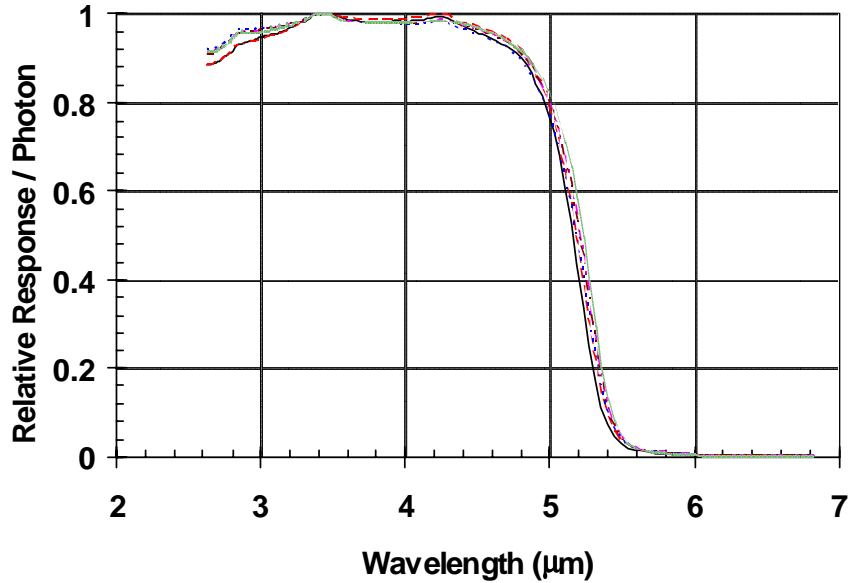


Figure 6. Spectral response of a typical MWIR HgCdTe detector showing relative QE plotted against wavelength. The absolute QE at the peak is 80% for this non-AR coated detector.

### 2.3 InSb detectors

InSb is a mature detector technology that has been demonstrated in arrays up to a 2048 x 2048 format.<sup>2,3</sup> The natural spectral response of InSb extends from 0.4 to 5.5 μm. Hyperspectral experiments, such as HYDICE, have successfully utilized InSb down to 0.4 μm. For astronomy and other low-background applications, InSb is generally used from 0.6 or 1.0 out to 5 μm. Two plots of QE as a function of wavelength are shown in Figure 7. One plot shows the response of a 1024 x 1024 InSb SCA with a single-layer AR coat measured by Fowler (NOAO) at seven wavelengths. The other plot shows measurements on a 2048 x 2048 InSb SCA with a seven-layer AR coat by McMurtry (University of Rochester) taken at eight discrete wavelengths. Both of these measurements show QEs ranging from 80% to 98%, depending on the wavelength and coating, from 0.6 to 5 μm.

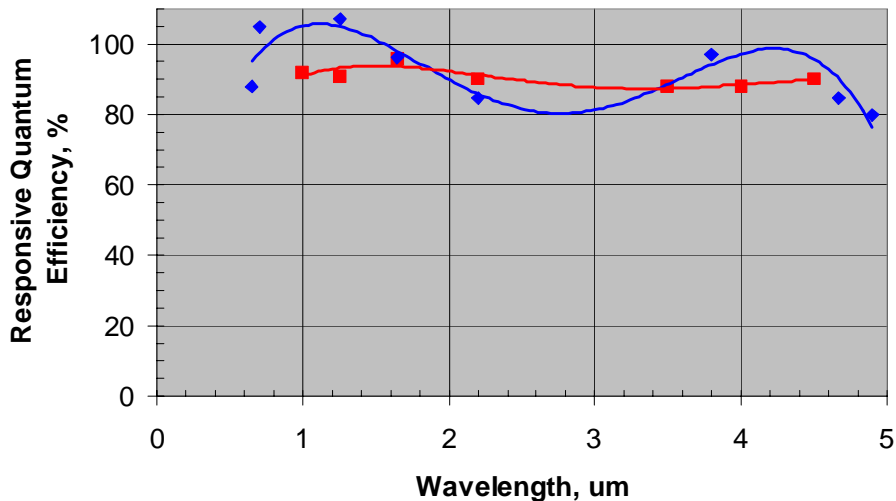


Figure 7. Spectral response of InSb SCAs showing absolute responsive QE as a function of wavelength. The squares are data obtained by A. Fowler of NOAO on a single-layer AR-coated 1024 x 1024 Aladdin InSb SCA. The diamonds are data obtained by C. McMurtry of University of Rochester on a seven-layer AR-coated 2048 x 2048 Phoenix InSb SCA.

Noise and dark current on large format InSb SCAs has been excellent. A 2048 x 2048 InSb SCA demonstrated 0.01e-/sec dark current at 30K and had a total noise (readout, detector, test system) of 6.2e- rms in 1000 s integration time with Fowler-8 sampling.<sup>2</sup> A photograph of this SCA, called Phoenix, is shown in Figure 8. It is a 3-side buttable device that allows a 2 by N focal plane to be constructed without large gaps in the active detector elements. A version of the 2048 x 2048 InSb SCA, called Orion and shown in Figure 9, has been developed specifically for ground-based astronomy where higher frames rates are required. This SCA has 64 output lines to increase the overall data rate.<sup>3</sup>

InSb SCAs have been successfully developed for NASA's Space Infrared Telescope Facility (SIRTF) and Japan's Astro-F mission. Both of these cooled space astronomy telescopes should launch in the next few months.

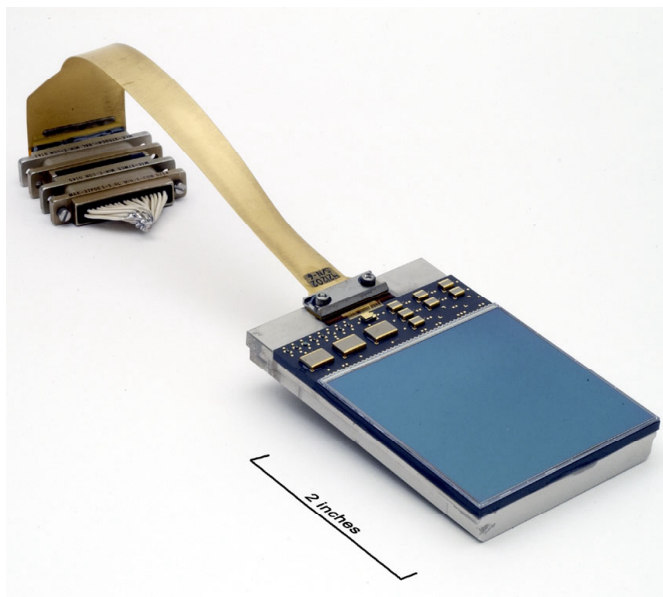


Figure 8. Photo of a 2048 x 2048 Phoenix InSb SCA on a module. The module consists of a precision metal pedestal to which a ceramic motherboard and SCA are attached. Noise-reducing capacitors and resistors are bonded to the motherboard along with a temperature sensor. A ribbon cable with low thermal conductivity provides the electrical interface.

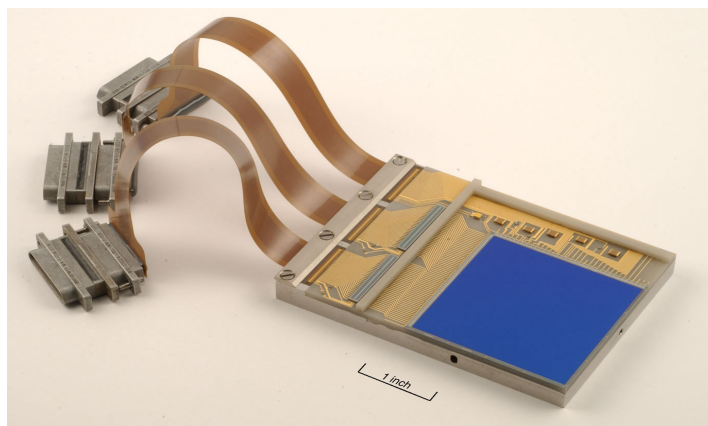


Figure 9. Photo of a 2048 x 2048 Orion InSb SCA on a module. The module consists of a precision metal pedestal to which a ceramic motherboard and SCA are attached. Noise-reducing capacitors and resistors are bonded to the motherboard along with a temperature sensor and current sources for the 64 outputs. Three ribbon cables provide the electrical interface, one for module operation and two for the output lines.

#### 2.4 Si:As IBC detectors

For long-wave detection in low-background systems the detector material with the highest performance is Si:As IBC. A typical spectral response of Raytheon's Si:As IBC detectors is shown in Figure 10. Two response curves are shown: one where the reflection loss at the incident surface has been removed (no reflection loss), and the other with a single-layer AR coating whose peak is at 6  $\mu\text{m}$ . Extremely low dark currents have been measured by Raytheon on a 1024 x 1024 Si:As IBC SCA: 0.05e-/s at 7K with a 1 volt reverse bias applied to the detectors.

Although 2048 x 2048 Si:As IBC SCAs would be easily produced with current technology, the largest array tested to date is 1024 x 1024. Figure 11 shows the 1024 x 1024 Si:As SCA that has recently been selected for the MIRI instrument on the James Webb Space Telescope (JWST).

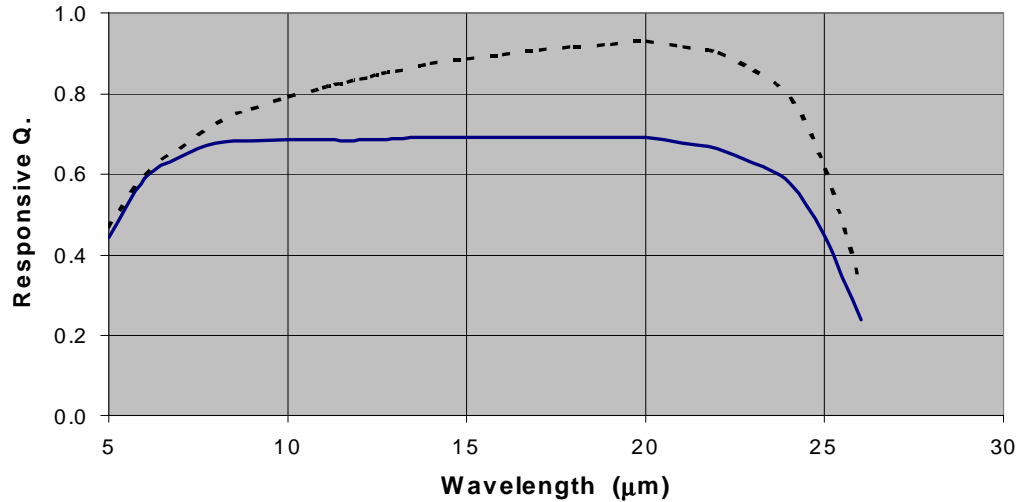


Figure 10. Spectral response of a typical Si:AS IBC detector showing responsive QE plotted against wavelength. The dashed curve is the internal QE, assuming no reflection loss. The solid curve is the QE with a single-layer AR-coating peaked at 6  $\mu\text{m}$ .

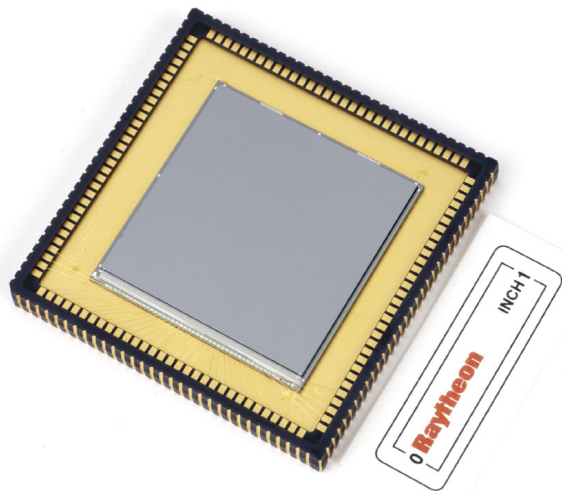


Figure 11. Photo of a 1024 x 1024 Si:As IBC SCA. This SCA has been selected for the MIRI instrument on JWST.

### 3. READOUT CHARACTERISTICS

A number of large-format high-performance readouts are available for low-background applications. A summary of readouts with 1024 x 1024 and 2048 x 2048 formats are shown in Table 1. Each of the readouts can be mated with any of the previous detectors. The MIRI readout has been optimized for 7K operation but also operates well at higher temperatures. The first column in Table 1 lists the name of each readout design and is also the name of any SCA fabricated from this readout. The next three columns show the format size, detector spacing, and the number of outputs, respectively. The last column provides the maximum frame rate at which each readout can operate. Note that there is a noise penalty for operating at higher frame rates that goes roughly as the square root of the frame rate.

This family of readouts has several design features in common. All readouts use the source-follower per detector (SFD), also called the self-integrator, as the input circuit that interfaces to the detector elements. All except the Aladdin chip have built-in reference pixels to help subtract off drift effects. For Aladdin, reference pixels can be generated using the "clamp" circuit. Finally, all readouts except Virgo have independent row and column shift registers (x-y addressing) to aid in quickly clocking out partial frames.

Table 1. A summary of large-format readouts available to hybridize with any detector material. The table shows key readout features such as detector spacing, number of outputs, and maximum frame rate for each readout design.

Name	Format	Detector Spacing, $\mu\text{m}$	Number of Outputs	Maximum frame rate, Hz
Aladdin	1024 x 1024	27	32	20
MIRI	1024 x 1024	25	4	1
Phoenix	2048 x 2048	25	4	0.25
Orion	2048 x 2048	25	64	10
Virgo	2048 x 2048	20	4 / 16	1 / 4

### 4. FUTURE DEVELOPMENTS

Two trends are likely to continue in the area of large format arrays. Both of these trends are driven by the desire of the user communities to have more and more pixels on the focal plane. So naturally the first trend is to produce even larger format SCAs. The number of pixels per SCA has approximately doubled every 18 months for the past 23 years, as shown in Figure 12 for MWIR astronomy arrays. This trend would predict a 4K x 4K array as early as next year. Although funding constraints will probably delay the arrival of the 4K x 4K infrared array, it is certainly within our grasp.

The second trend that increases the number of pixels per focal plane, is the close-butted mosaic of several SCAs as shown in Figure 13. Although there are currently limitations to reducing the size of the gaps between active detectors on adjacent SCAs, many of these can be overcome. Focal planes of 100 megapixels and larger will be possible, constrained only by budgets, not technology.



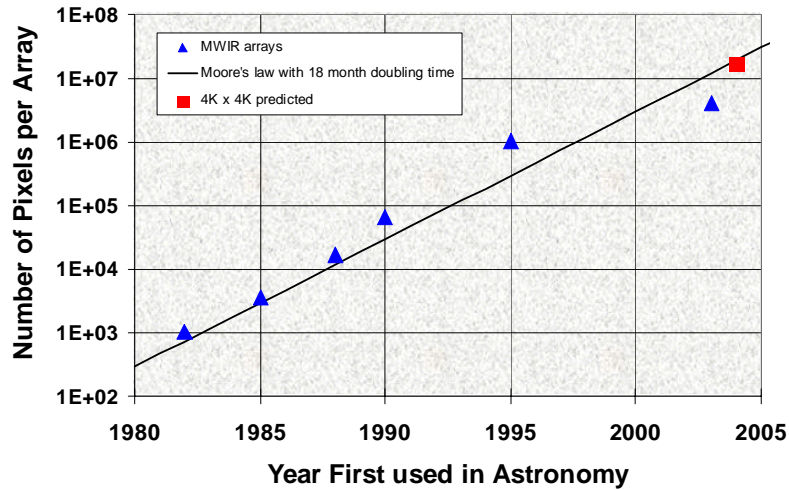


Figure 12. Array size continues to increase with an 18 month doubling time. The graph shows the low of the number of pixels per SCA as a function of the year first used in astronomy for MWIR SCAs. This exponential increase predicts a 4K x 4K MWIR SCA by 2004.

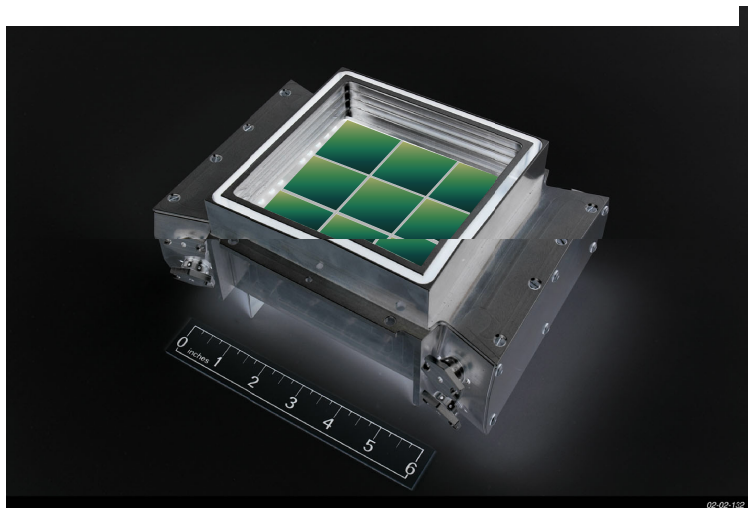


Figure13. A 3 x 3 focal plane concept with close-butted SCAs. The close assembly of many SCAs allows even more pixels on the focal plane.

## 5. ACKNOWLEDGMENTS

The authors thank the various astronomy groups that have tested these SCAs to their limits. In particular, we thank the University of Rochester, the National Optical Astronomy Observatories, the UK Astronomy Technology Centre, NASA Ames Research Center, and the Space Telescope Science Institute.

## 6. REFERENCES

1. P. J. Love, A. W. Hoffman, D. L. Gulbransen, K. J. Ando, M. P. Murray, N. J. Therrien, "Large-format 0.85 and 2.5  $\mu\text{m}$  HgCdTe detector arrays for low-background applications," in Proc. SPIE, Focal Plane Arrays for Space Telescopes, T. J. Grycewicz and C. R. McCreight, eds. 5167, these proceedings, 2-8 Aug. 2003.
2. C. W. McMurtry, W. J. Forrest, J. L. Pipher, A. C. Moore, "James Webb Space Telescope characterization of flight candidate NIR InSb array," in Proc. SPIE, Focal Plane Arrays for Space Telescopes, T. J. Grycewicz and C. R. McCreight, eds. 5167, these proceedings, 2-8 Aug. 2003.
3. K. M. Merrill, A. M. Fowler, W. Ball, A. Henden, F. J. Vrba, C. McCreight, "Orion II: the second-generation readout multiplexer for largest infrared hybrid focal plane," in Proc. SPIE, Focal Plane Arrays for Space Telescopes, T. J. Grycewicz and C. R. McCreight, eds. 5167, these proceedings, 2-8 Aug. 2003.